

RISØ

Polymeric Composites - Expanding the Limits

Editors

S.I. Andersen, P. Brøndsted, H. Lilholt, Aa. Lystrup

J.T. Rheinländer, B.F. Sørensen, H. Toftegaard

18th Risø International Symposium
on Materials Science
1997

Proceedings of the 18th Risø International Symposium on Materials Science:
Polymeric Composites - Expanding the Limits

Editors: S.I. Andersen, P. Brøndsted, H. Lilholt, Aa. Lystrup,
J.T. Rheinländer, B.F. Sørensen and H. Toftegaard.
Risø National Laboratory, Roskilde, Denmark, 1997

DYNAMIC MECHANICAL PROPERTIES OF THE SPHERICAL
INCLUSION- POLYMER COMPOSITES: CASE THE
COMPOSITES BASED ON UNTREATED, AMINOSILANE-
TREATED AND ELASTOMER COATED FILLERS

M. Shaterzadeh⁽¹⁾, J.F. Gerard⁽²⁾, C. Mai⁽¹⁾ and J. Perez⁽¹⁾

⁽¹⁾ Lab. GEMPPM, UMR 5510, CNRS, INSA de Lyon, 20 Av. Albert
Einstein, F-69621 Villeurbanne Cedex, France

⁽²⁾ Lab. LMM, UMR 5627, CNRS, INSA de Lyon, 20 Av. Albert
Einstein, F-69621 Villeurbanne Cedex, France

ABSTRACT

The *Self-Consistent Scheme* was used to predict the dynamic mechanical properties of the composites. Three types of the composites (polyepoxy matrix) were studied with, (i) non treated fillers, (ii) aminosilane-treated fillers, and (iii) elastomer coated fillers. In the case of the composites based on untreated and aminosilane-treated fillers, the $(n+1)$ phase model developed by Hervé and Zaoui was chosen. The problem for 3 phases was solved by modifying it: (i) with considering the spatial distribution of glass particles and, (ii) with repeating the self-consistent model. In the case of the composites with elastomeric interlayer, the 4 phase model was used by taking into account the changing of the interlayer's properties. Conditions of linear elasticity were assumed and the Poisson's coefficient was considered to vary from 0.32 in the glassy state to 0.5 in the rubbery state. The theoretical results well fit the experimental data.

1. INTRODUCTION

Particulate composites are generally used as model systems for studying the mechanical behaviour of composites in which the filler has a more complex geometry (Nielsen 1970, 1994). The comparison of the differences between theoretical models and experimental results for dynamic mechanical properties of particulate reinforced polymers is one of the limitations for understanding of the effect of the role of each component, i.e. the filler, the matrix, and the interface or interphase. Several micro-mechanical models were proposed to predict the dynamic mechanical properties of these composite materials: Geometric, i.e. Kerner (1956), Self-Consistent, i.e. Hill (1965), or variational models, i.e. Hashin and Shtrikman (1963).

In order to study the elastic behaviour of two phases matrix-inclusion composites, Christensen and Lo (1986), and Hervé and Zaoui (1993) proposed a *Generalised Self-Consistent Scheme* describing the material from the micro to macro scale.

In such an approach the system is considered as a spherical inclusion surrounded by a matrix shell which in turn is surrounded by the effective equivalent medium (Fig. 1). In this paper, we attempt to compare theoretical and experimental dynamic mechanical properties by carrying out measurements on a cross linked polymer (epoxy) reinforced with three types of spherical A-glass particles using a low frequency torsion pendulum operating in forced oscillations.

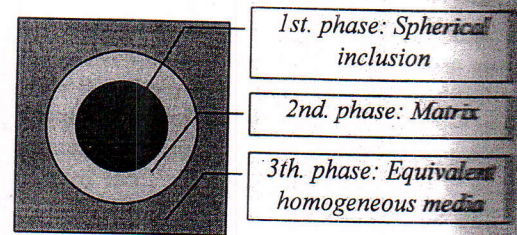


Fig. 1. Three phase model

2. EXPERIMENTAL PROCEDURE

Composites specimens based on a polyepoxy matrix filled with 10%, 20%, 30%, and 50% volume fraction of untreated, aminosilane(γ APS)-treated, and elastomer coated A-glass beads were prepared. The average particle sizes of the A-glass spheres were 40 μm (in number). The epoxy network was synthesized from an epoxy prepolymer (DGEBA) and a primary diamine comonomer (IPD), considering a stoichiometric ratio (amino-hydrogen to epoxy) equal to 1. The interlayer that is coated the fillers, was a elastomer (DGEBA-CTBN-IPD).

Dynamic mechanical spectrometry was carried out using an inverted torsion pendulum. This apparatus allowed the investigation of the dynamic mechanical behaviour of materials, such as the storage shear modulus, G' , and the loss modulus, G'' , and the internal friction $\tan \delta = G''/G'$ (loss tangent) as a function of temperature. Parallelepipedic specimens (55*6*2 mm³) were machined from the casted plates. Measurements were performed from 100K to 464K at a frequency of 1Hz.

3. RESULTS, MODELISATION AND DISCUSSION

3.1. Dynamics mechanical spectra of neat epoxy and non treated filler's composites.

Fig. 2 displays the isochronal experimental plots of G' by increasing the temperature from 100K to 464K for the neat matrix and the composites based on various volume fractions of glass beads (10%, 20%, 30%, and 50%).

The Table 1, reports values obtained for neat matrix and the composite materials. These results show that with increasing the volume fraction of filler, the magnitude of the mechanical relaxation (the $\tan \delta$ value at the maximum) decreases and the temperature position of the α peak is slightly shifted towards higher temperatures. The storage modulus, G' , increases, where as the shear modulus in the rubbery state (G' at $T=464\text{K}$) is highly enhanced with increasing the filler content.

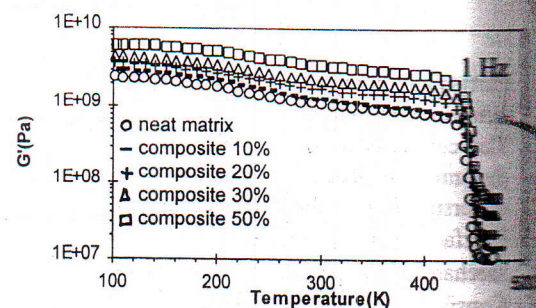


Fig. 2. Experimental results of G' modulus

Dynamic mechanical properties of the spherical inclusion composites

Table 1: Dynamic mechanical properties of the neat matrix and composites materials based on various volume fractions of untreated glass beads (Experimental data)

	$T\alpha$ (K)	$\tan(\delta)_{max}$	G' (MPa) (at $T=100K$)	G' (MPa) (at $T=464K$)	G'' (MPa) (at $T=300K$)
Matrix DGEBA/IPD	446	1.08	2450	10.8	28.5
Composite 10%	447	1	3040	14.3	33.4
Composite 20%	448	0.969	3690	21.4	41.9
Composite 30%	449	0.879	4460	38.9	51.7
Composite 50%	449	0.782	6740	66.6	62.3

3.2. Modelling the DMS Behaviour. Hervé and Zaoui (1993) generalized and determined the effective shear and bulk modulus of the composites. This analysis consists of the single composite sphere embedded in an infinite medium (Fig. 1) of unknown effective properties. This model requires that the effective homogeneous medium has the same average conditions of stress and strain as for the spherical model described in Fig. 1. After some calculations (Hervé 1993) in the case of a simple shear deformation, and by considering the correspondence between the elastic (G_c) and the viscoelastic (G_c^*) (Hashin 1970), the final equation for dynamic shear modulus of composite (G_c^*) is given by the following second order equation:

$$A\left(\frac{G_c^*}{G_m^*}\right)^2 + B\left(\frac{G_c^*}{G_m^*}\right) + C = 0 \quad (1)$$

where A, B, and C are constants and G_m^* is the dynamic shear moduli of the matrix (Appendix).

3.3. Untreated glass bead's composites: Comparison between experimental and theoretical dynamic mechanical behaviours : For a low volume fraction of filler ($\phi_f \leq 20\%$), the fillers are well dispersed in the matrix and the calculated results are well fitted by the experimental data. But for the composites with a higher volume fraction of glass beads ($\phi_f > 20\%$), this model can not described correctly the experimental data. Indeed, as shown in the Fig. 3, the experimental shear modulus, in the rubbery state, for a composite based on 30% vol. of glass beads, is not well fitted by the model. The main reason of the difference between experimental and calculated results is due to the real morphology of the composite. The micrography of composite shows, there is an agglomeration of particles. So two parameters need to be considered: (i) the Poisson's coefficient of the matrix which is not constant from the glassy to the rubbery state and; (ii) the morphology of the material, i.e. the spatial distribution of filler.

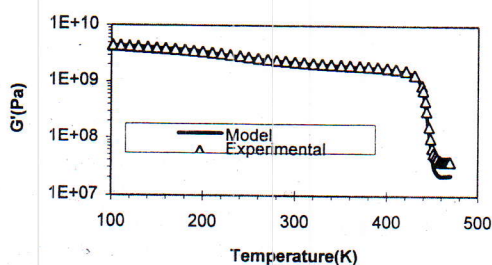


Fig. 3. Storage shear modulus of a composite based on 30% vol. of glass.

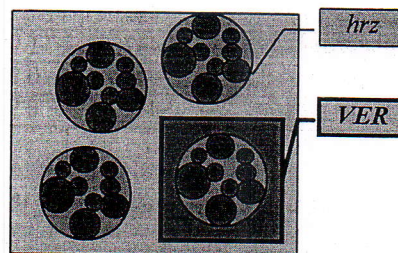


Fig. 4. Scheme of the particles' agglomeratin and spherical composite inclusions (hrz)

To take into account of the morphology, the volume element representative (VER) is considered as in Fig. 4. Thus, *highly reinforced zones (hrz)* are defined as the zone in the composite with a higher volume fraction of glass beads, ϕ_{hrz} , than the average one, ϕ_f . The problem was then solved in two steps; (i) in the first step, the dynamic mechanical properties of the highly reinforced zone are calculated and, (ii) in the second step the properties of the equivalent homogeneous media or whole composite are calculated (Fig. 5).

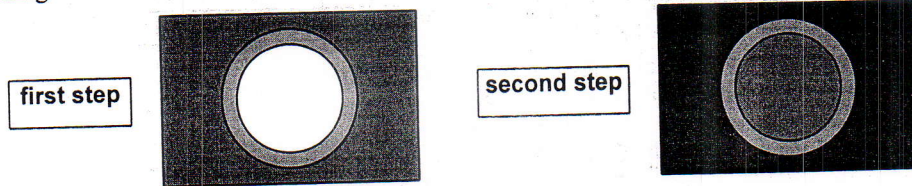


Fig.5. Three phase model of solution in the two step calculation

In this two step analysis, the Poisson's coefficient is considered as temperature dependent. The value of ϕ_{hrz} is an important parameter and it can be given by measuring the volume fraction of glass beads in these highly reinforced composite. The final calculated behaviour for a composite based on 30% vol. of glass with ϕ_{hrz} equal to 51% is given in Fig. 6.

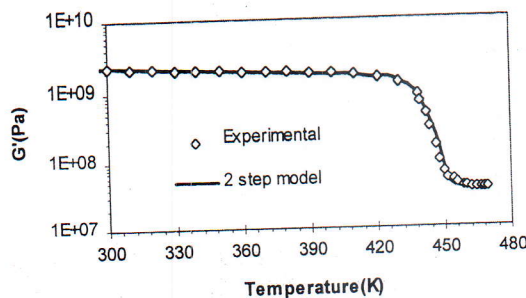


Fig. 6. Calculated results(2-steps, and $\phi_{hrz}=51\%$) given by modified Hervé's model for a composite based on 30% vol. of untreated glass beads.

This hypothesis are confirmed for the composite with a higher volume fraction of glass. (50% vol.). Table 2 shows the best calculated fittings of the dynamic mechanical properties of composite material based on different glass bead contents.

Table 2: Calculated optimized characteristics, for composites based on the various volume fraction of untreated glass beads

	$T\alpha$ (K)	$\tan(\delta)_{max}$	$G'(MPa)$ (at $T=100K$)	$G'(MPa)$ (at $T=464K$)	$G''(MPa)$ (at $T=300K$)
Composite 10%	446	1.08	2988	14.3	35.8
Composite 20%	447	1.006	3701	20.12	45.5
Composite 30%	448	0.989	4452	39.2	57.5
Composite 50%	448	0.985	6614	64.2	79.5

Fig. 7 shows the calculated results using Kerner's and Hervé -Zaoui's models in comparison with experimental data. One notice that in the rubbery state, the Kerner's model has a very bad fit.

3.4. Comparison between experimental and theoretical dynamic mechanical behaviours for the aminosilane-treated glass bead composites. In the second type of the composites, micrography observation shows, there is not the high agglomeration of the fillers and the homogeneity of the composites are better.

Dynamic mechanical properties of the spherical inclusion composites

In this case the calculated volume fraction of highly reinforced zone, ϕ_{hrz} , equal to 37% instead of 51% in the untreated filler composite (30%). In the other hand we can consider that the glass particles are better dispersed. So for predicting the dynamic behaviour of these composites, we can use the same model with only one step of calculation (Fig. 8).

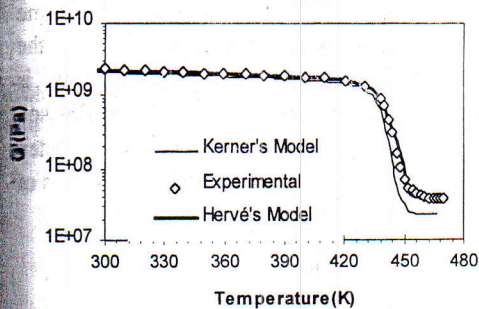


Fig. 7. Comparison of the calculated results (2 step, v variable, $\phi_{hrz}=51\%$) by Hervé and Kerner's model

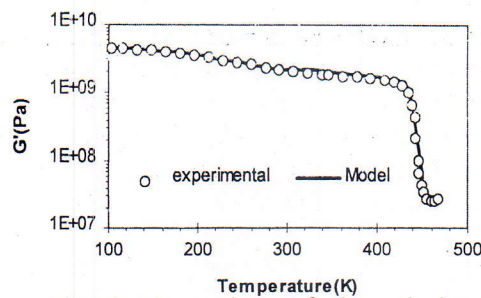


Fig. 8. Comparison of the calculated results (1 step, v variable,) and experimental results for the composite based on 30% vol. treated glass beads.

3.5. Comparison between experimental and theoretical dynamic mechanical behaviours for the elastomer coated glass bead composites. In the case of the composites with interlayer ($e/r=1.5\%$, e : thickness of the interphase and r : the radiate of the filler), the distribution of glass particles (observed by microscopy), is homogenate. The same model with 4 phases (1. filler, 2. interlayer, 3. matrix, 4. equivalent homogeneous media), in one step is used (Fig. 9), but the calculated curve is not fitted by the experimental once (Fig. 10 (a)). The reason of this difference should be the change of the interlayer's properties.

Indeed the T_α of the elastomeric material in comparison with the matrix (Epoxy) is very lower ($T_\alpha=240K$), but in the composite's interlayer (interphase), the molecular mobility reduce and it has not the same behaviour. So we have supposed that the storage modulus (G') of the interlayer (interphase) is between the G' of the elastomer material and G' of the matrix (Epoxy). So with this hypothesis, the calculated results show a best fitting with the experimental data (Fig. 10 (b)).

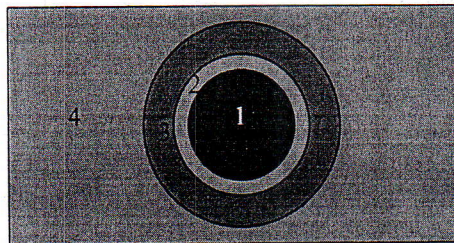


Fig. 9. Four phases model of solution for the composite with interlayer

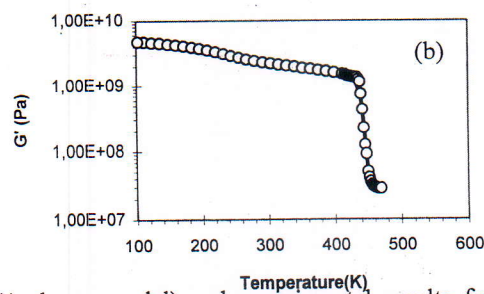
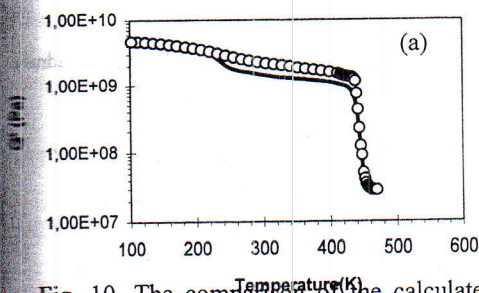


Fig. 10. The comparison of the calculated (4 phases model) and experimental results for composite 30% with non (a) non modified interphase and, (b) modified interphase properties.

4. CONCLUSION

In this work we have shown that in the case of low volume fraction of the filler, the self-consistent models developed by Christensen-Lo and Hervé- Zaoui, predict a better fitting for dynamic behaviour of the particulate composite than Kerner's one. But in the higher volume fraction of glass beads ($\phi_p > 20\%$), these models can not well predict the dynamic properties in the glass transition region especially in the rubbery state. So the model of Hervé and Zaoui, is modified by including the real morphology of the composite and, the variation of the Poisson ratio. In the case of the composites with interlayer (interphase), a 4 phases model in one step describe correctly the properties of the composite, but it must be considered that the properties of the interphase i.e. G' , change between the matrix and interlayer's values.

REFERENCES

- Agbossou, A., Bergeret, A., Benzarti, K. and Alberola, N. (1993). A modelling of the viscoelastic behaviour of amorphous thermoplastic/glass beads composites based on the evaluation of the complex Poisson's ratio of the polymer matrix. *J. Mat. Sci.*, **28**, 1963-1972.
- Christensen, R.M., and Lo, K.H. (1986). Solutions for effective shear properties in three phases sphere and cylinder models. *J. Mech. Phys. Solids*, **27**, p.315. (1979). Erratum **34**, p.639.
- Hashin, Z., and Shtrikman S. (1963). A variational approach to the theory of the elastic behaviour of multiphase materials. *J. Mech. Phys. Solids*, **11**, p.127.
- Hashin, Z. (1970). Complex moduli of viscoelastic composites. II. Fibre reinforced materials. *J. Solids Structures*, **6**, 797-807.
- Hervé, E., and Zaoui, A. (1993). n-Layered inclusion-based micromechanical modelling. *Int. J. Engng Sci.*, **31**(N°1), 1-10.
- Hill, R. (1965). Theory of mechanical properties of fibre-strengthened materials-III. Self-consistent model. *J. Mech. Phys. Solids*, **13**, 189-198.
- Kerner, E.H. (1956). The elastic and thermo-elastic properties of composite media. *Proc. Roy. Soc. Lond.*, **69B**, 808-813
- Lewis, T.B., and Nielsen, L.E. (1970). Dynamic mechanical properties of particulate -filled composites. *J. Appl. Polym. Sci.*, **14**, 1449-1471.
- Nielsen, A.E., and Landel, R.F. (1994). *Mechanical Properties of Polymers and Composites*. Dekker, New York, 557pp.
- Shaterzadeh, M., Gerard, J.F., Mai, C., and Perez, J. (1996). Dynamic Mechanical Properties of Spherical Inclusions in Polymer Composite: A Self Consistent Approach Considering Morphologie. *J. Poly.Composite*. Submitted.

APPENDIX

The final solution from Herve and Zaoui for G^* of the particulate composite is given by the results of the quadratic equation (A-1):

$$A \left(\frac{G_c^*}{G_m^*} \right)^2 + B \left(\frac{G_c^*}{G_m^*} \right) + C = 0 \quad (A-1)$$

where, A, B, and C are constants. For three phase model, the following simplified expressions are:

$$A = 4R_2^{10} (1 - 2v_m)(7 - 10v_m)H_{12} + 20R_2^7 (7 - 12v_m + 8v_m^2)H_{42} + 12R_2^5 (1 - 2v_m) \times (H_{14} - 7H_{23}) + 20R_2^3 (1 - 2v_m)^2 H_{13} + 16(4 - 5v_m)(1 - 2v_m)H_{43} \quad (A-2)$$

Dynamic mechanical properties of the spherical inclusion composites

$$B = 3R_2^{10}(1-2\nu_m)(15\nu_m-7)H_{12} + 60R_2^7(\nu_m-3)\nu_m H_{42} - 24R_2^5(1-2\nu_m) \times (H_{14} - 7H_{23}) - 40R_2^3(1-2\nu_m)^2 H_{13} - 8(1-5\nu_m)(1-2\nu_m)H_{43} \quad (A-3)$$

$$C = -R_2^{10}(1-2\nu_m)(7+5\nu_m)H_{12} + 10R_2^7(7-\nu_m^2)H_{42} + 12R_2^5(1-2\nu_m) \times (H_{14} - 7H_{23}) + 20R_2^3(1-2\nu_m)^2 H_{13} - 8(7-5\nu_m)(1-2\nu_m)H_{43} \quad (A-4)$$

which, $R_2=1$ and $H_{n\beta}$ are the products of the members of the following matrix P, thus $\eta(\beta)$ are the number of line (column) of the matrix P:

$$\begin{aligned} H_{12} &= P_{1,1} \cdot P_{2,2} - P_{2,1} \cdot P_{1,2} \\ H_{13} &= P_{1,1} \cdot P_{3,2} - P_{3,1} \cdot P_{1,2} \\ H_{14} &= P_{1,1} \cdot P_{4,2} - P_{4,1} \cdot P_{1,2} \\ H_{23} &= P_{2,1} \cdot P_{3,2} - P_{3,1} \cdot P_{2,2} \\ H_{42} &= P_{4,1} \cdot P_{2,2} - P_{2,1} \cdot P_{4,2} \\ H_{43} &= P_{4,1} \cdot P_{3,2} - P_{3,1} \cdot P_{4,2} \end{aligned}$$

with matrix of P:

$$P = \frac{1}{5(1-\nu_m)} \begin{bmatrix} \frac{c}{3} & \frac{R_1^2(3b-7c)}{5(1-2\nu_f)} & \frac{-12\alpha}{R_1^5} & \frac{4(f-27\alpha)}{15(1-2\nu_f)R_1^3} \\ 0 & \frac{(1-2\nu_m)b}{7(1-2\nu_f)} & \frac{-20(1-2\nu_m)\alpha}{7R_1^7} & \frac{-12\alpha(1-2\nu_m)}{7(1-2\nu_f)R_1^5} \\ \frac{R_1^5\alpha}{2} & \frac{-R_1^7(2a+147\alpha)}{70(1-2\nu_f)} & \frac{d}{7} & \frac{R_1^2[105(1-\nu_m)+12\alpha(7-10\nu_m)-7e]}{35(1-2\nu_f)} \\ -\frac{5}{6}(1-2\nu_m)\alpha R_1^3 & \frac{7(1-2\nu_m)\alpha R_1^5}{2(1-2\nu_f)} & 0 & \frac{e(1-2\nu_m)}{3(1-2\nu_f)} \end{bmatrix}$$

with:

$$a = \left(\frac{G_f^*}{G_m^*} \right) \cdot (7+5\nu_f) \cdot (7-10\nu_m) - (7-10\nu_f) \cdot (7+5\nu_m)$$

$$b = 4(7-10\nu_f) + \left(\frac{G_f^*}{G_m^*} \right) \cdot (7+5\nu_f)$$

$$c = (7-5\nu_m) + 2 \left(\frac{G_f^*}{G_m^*} \right) \cdot (4-5\nu_m)$$

$$d = (7+5\nu_m) + 4 \left(\frac{G_f^*}{G_m^*} \right) \cdot (7-10\nu_m)$$

$$e = 2(4-5\nu_f) + \left(\frac{G_f^*}{G_m^*} \right) \cdot (7-5\nu_f)$$

$$f = (4-5\nu_f) \cdot (7-5\nu_m) - \left(\frac{G_f^*}{G_m^*} \right) \cdot (4-5\nu_m) \cdot (7-5\nu_f)$$

$$\alpha = \left(\frac{G_f^*}{G_m^*} \right) + 1$$